SISSA

**PAPER • OPEN ACCESS**

# The SIDDHARTA-2 Veto-2 system for X-ray spectroscopy of kaonic atoms at DAΦNE

# The SIDDHARTA-2 Veto-2 system for X-ray spectroscopy of kaonic atoms at DAΦNE

M. Tüchler,[a,*] C. Amsler,[a] M. Bazzi,[b] D. Bosnar,[c] M. Bragadireanu,[d] M. Cargnelli,[a]
M. Carminati,[e,f] A. Clozza,[b] G. Deda,[e,f] R. Del Grande,[b,g] L. De Paolis,[b] K. Dulski,[b]
L. Fabbietti,[g] C. Fiorini,[e,f] I. Friščić,[c] C. Guaraldo,[b] M. Iliescu,[b] M. Iwasaki,[h] A. Khreptak,[b]
S. Manti,[b] J. Marton,[a] M. Miliucci,[b] P. Moskal,[i,j] F. Napolitano,[b] S. Niedźwiecki,[i,j]
H. Ohnishi,[k] K. Piscicchia,[l,b] Y. Sada,[j] A. Scordo,[b] F. Sgaramella,[b] H. Shi,[a] M. Silarski,[i]
D. Sirghi,[b,d,l] F. Sirghi,[b,d] M. Skurzok,[i,j] A. Spallone,[b] K. Toho,[k] O. Vazquez Doce,[b]
E. Widmann,[a] C. Yoshida,[k] J. Zmeskal[a] and C. Curceanu[b]

[a]Stefan-Meyer-Institut für Subatomare Physik,
Dominikanerbastei 16, 1010 Vienna, Austria

[b]Laboratori Nazionali di Frascati INFN,
Via E. Fermi 54, 00044 Frascati, Italy

[c]Department of Physics, Faculty of Science, University of Zagreb,
Bijenicka cesta 32, 10000 Zagreb, Croatia

[d]Horia Hulubei National Institute of Physics and Nuclear Engineering (IFIN-HH),
Reactorului 30, 077125 Magurele, Romania

[e]Politecnico di Milano, Dipartimento di Elettronica, Informazione e Bioingegneria
and INFN Sezione di Milano,
Piazza Leonardo da Vinci 32, 20133 Milano, Italy

[f]INFN Sezione di Milano,
Via Celoria 16, 20133 Milano, Italy

[g]Physik Department E62, Technische Universität München,
James-Franck-Straße 1, 85748 Garching, Germany

[h]RIKEN,
2-1 Hirosawa, Wako, Saitama, 351-0198 Tokyo, Japan

[i]Faculty of Physics, Astronomy, and Applied Computer Science, Jagiellonian University,
Łojasiewicza 11, 30-348 Krakow, Poland

[j]Center for Theranostics, Jagiellonian University,
Krakow, Poland

[k]Research Center for Electron Photon Science (ELPH), Tohoku University,
982-0826 Sendai, Japan

[l]Centro Ricerche Enrico Fermi – Museo Storico della Fisica e Centro Studi e Ricerche "Enrico Fermi",
Via Panisperna 89A, 00184 Roma, Italy

E-mail: marlene.tuechler@oeaw.ac.at

---

*Corresponding author.

ABSTRACT: The Veto-2 is a fundamental component of a multiple-stage veto system for the SIDDHARTA-2 experiment installed at the DAΦNE collider at INFN-LNF in Italy. It was developed to improve the signal-to-background ratio for the challenging measurement of X-ray transitions to the fundamental level in kaonic deuterium. Its purpose is the suppression of hadronic background in the form of Minimum Ionizing Particles by using the topological correlation between signals in the X-ray and Veto-2 detectors. The Veto-2 system consists of a barrel of plastic scintillators read out by Silicon Photomultipliers. The system performed its first successful test run within the apparatus with a helium-4 target in 2022. The efficiency of the Veto-2 was determined and found to be $0.62 \pm 0.01$. The Veto-2 improved the signal-to-background ratio for the kaonic helium-4 $L_\alpha$ measurement by $\sim 16\%$, which is crucial due to the low expected X-ray yield of kaonic deuterium.

## Contents

## 1 Introduction

The SIDDHARTA-2 experiment, installed at the DAΦNE collider at INFN-LNF in Italy, performs X-ray spectroscopy of kaonic deuterium (K⁻d) atoms to measure transitions to the fundamental level. These results will, in combination with the kaonic hydrogen (K⁻p) measurement [1], allow to obtain the antikaon-nucleon scattering lengths and to advance the understanding of the low-energy antikaon-nucleon interaction with strangeness. DAΦNE, an e⁺e⁻ collider operating at the centre-of-mass energy of the $\phi$-meson at 1.02 GeV, represents a unique source of monochromatic charged kaon pairs with low momentum (127 MeV/c [2]). X-ray spectroscopy of kaonic deuterium poses an even bigger experimental challenge than that of kaonic hydrogen due to several factors: the low X-ray yield, which is expected to be one order of magnitude smaller than for kaonic hydrogen [3–6], and the broad width of the K⁻d $1s$ level in kaonic deuterium (expected to be $\sim 1000$ eV and thus twice as large as for kaonic hydrogen [7–11]), in combination with a high-radiation background present at DAΦNE. Therefore, several methods are utilised in the apparatus to increase the signal-to-background ratio (S/B) by at least one order of magnitude compared to the K⁻p measurement. The first one is the implementation of a lightweight, gaseous target cell for the formation of the kaonic atoms. Secondly, a new X-ray detection system made of Silicon Drift Detectors (SDDs) was developed [12–15]. The new SDDs have a smaller active area of $8 \times 8$ mm² each compared to the ones of the K⁻p measurement, leading to an improvement of the drift time from approximately 800 ns to approximately 450 ns. Thirdly, a multiple-stage veto system was implemented for the active suppression of the synchronous background. The purpose of the first veto stage (Veto-1) is the reduction of background originating from kaons stopping in the solid support structures of the setup instead of in the gaseous target via timing information [16]. The second stage and focus of this paper, the Veto-2 system, suppresses background from Minimum Ionizing Particles (MIPs) passing through the X-ray detectors. The MIPs are produced in the absorption of the kaons on the nucleons of the target after the formation of a kaonic atom. They can create a signal in the region of interest (ROI) for K⁻d X-rays (5–15 keV), depending on their path through the SDDs, as shown in figure 1. A MIP traversing the detector on the edge of its active area deposits less energy than a central hit.

This is also the case for secondary X-rays or backscattered electrons crossing the X-ray detectors. This source of background is eliminated by using the topological correlation between signals in the SDDs and signals in the corresponding Veto-2 detectors.

The Veto-2 system further provides timing information which is useful for the characterisation of the background present during data acquisition, as well as the optimisation of the setup.

The SIDDHARTA-2 experiment performed its first successful measurements including the complete veto systems with a helium-4 target in 2022. In this paper, a detailed description of the method of background reduction, timing performance, and efficiency of the Veto-2 system is presented. More details can be found in [17].
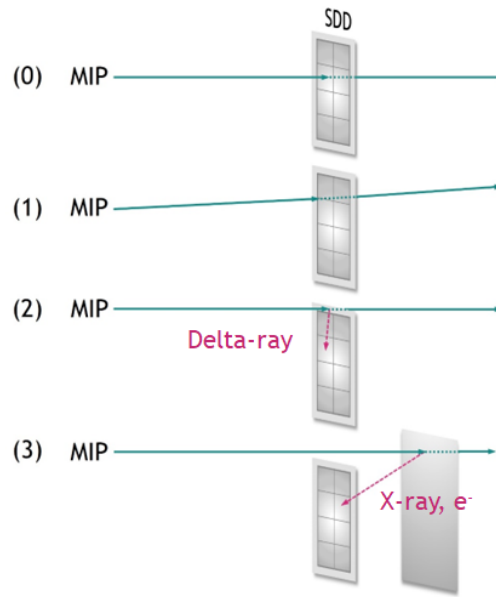


**Figure 1**. Motivation for the Veto-2 system: (0) Most frequent case in which the MIP passes through the centre of the SDD active area, producing a large signal; (1) The MIP passes the SDD through the edge of its active area, producing a signal in the ROI. (2) Delta-rays, (3) backscattered electrons or secondary X-rays produced in the setup pass through the SDD.

## 2 Veto-2 detector design and experimental apparatus

The Veto-2 system consists of 24 units. Each unit contains four detectors; one detector consists of a $12 \times 5 \times 50 \, \text{mm}^3$ EJ-200 plastic scintillator and a Silicon Photomultiplier (SiPM) with an active area of $4 \times 4 \, \text{mm}^2$. The SiPMs were produced by AdvanSiD in Trento, Italy, and operate in the near-UV range with a peak sensitivity wavelength of 420 nm [18]. Figure 2(a) shows the schematics of one Veto-2 unit. To minimise the crosstalk between the four detectors in the same unit, the scintillators are wrapped in Teflon tape.

Since the detectors are mounted in a high-radiation environment, a calibration system based on pulsed LEDs is implemented to monitor their performance in-situ. The LEDs are placed between two SiPMs (see figure 2(b)), resulting in a total of 48 LEDs for the full system. Eight LEDs are supplied in parallel by a pulse generator developed and constructed at Stefan Meyer Institute in Vienna,

which provides TTL pulses with a frequency of 100 Hz and a pulse width of 126 ns. Dedicated amplification boards supply the bias voltage for the SiPMs and the amplification and front-end processing of their output signals [19]. Each board features sixteen input channels and a total of 32 output channels. For each input, there is one analogue and one digital output channel. The analogue output delivers the amplified voltage pulse of the SiPMs. The digital output provides a Low Voltage Differential Signal (LVDS) for the Time-over-Threshold (ToT) of the analogue pulse. The bias voltage of approximately 31 V for the SiPMs is provided by High-Voltage (HV) modules. The HV modules were updated to operate as constant-voltage sources, providing a constant overvoltage independent of the dark current. This update was crucial due to radiation damage to the SiPMs, as described in section 3. Figure 3 shows the block diagram of the HV module for one SiPM.
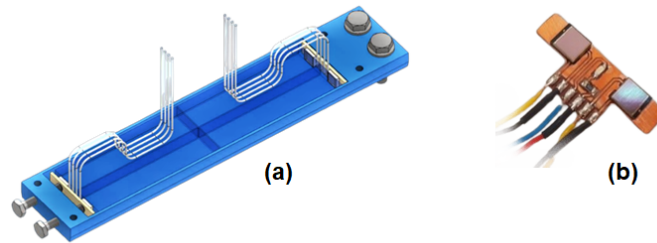


**Figure 2**. (a) Schematic drawing of a Veto-2 unit consisting of four scintillators and SiPMs. (b) Two SiPMs with a blue LED in-between, mounted on a printed board.
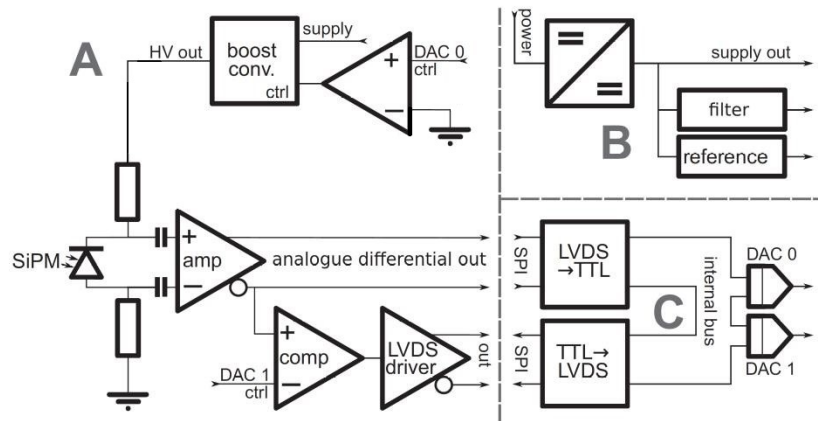


**Figure 3**. Block diagram of a HV module for the supply of a constant bias voltage to the SiPM [19, 20]. Reprinted from [19], Copyright (2016), with permission from Elsevier.

The Veto-2 system was installed in the SIDDHARTA-2 apparatus in 2022, located at the interaction point (IP) of the DAΦNE collider (figure 4). It performed its first cycles of operation during the spring and summer runs. A kaon trigger consisting of a pair of scintillators with photomultiplier readout, placed above and below the beam pipe, detects the back-to-back charged kaons from $\phi$-decay. A luminosity monitor provides real-time feedback of the beam quality and background conditions [21–25]. After passing through a thin kaon degrader, the negatively charged

kaon is stopped in the gaseous target cell and a kaonic atom is formed, whereas the positively charged kaon will not form a kaonic atom, but decay after its mean lifetime of 12.4 ns [26]. The X-rays emitted from the kaonic atoms are detected by the system of 48 arrays of SDDs surrounding the cylindrical target cell, with each array consisting of eight SDD cells. The Veto-2 system is mounted directly behind the SDDs. The Veto-1, a barrel of twelve plastic scintillators with photomultiplier readout, surrounds the vacuum chamber on its outside. Data were collected with a gaseous helium-4 target (1.1% Liquid Helium Density (LHeD)) for an integrated luminosity of $5\,\text{pb}^{-1}$ (corresponding to 3 days).
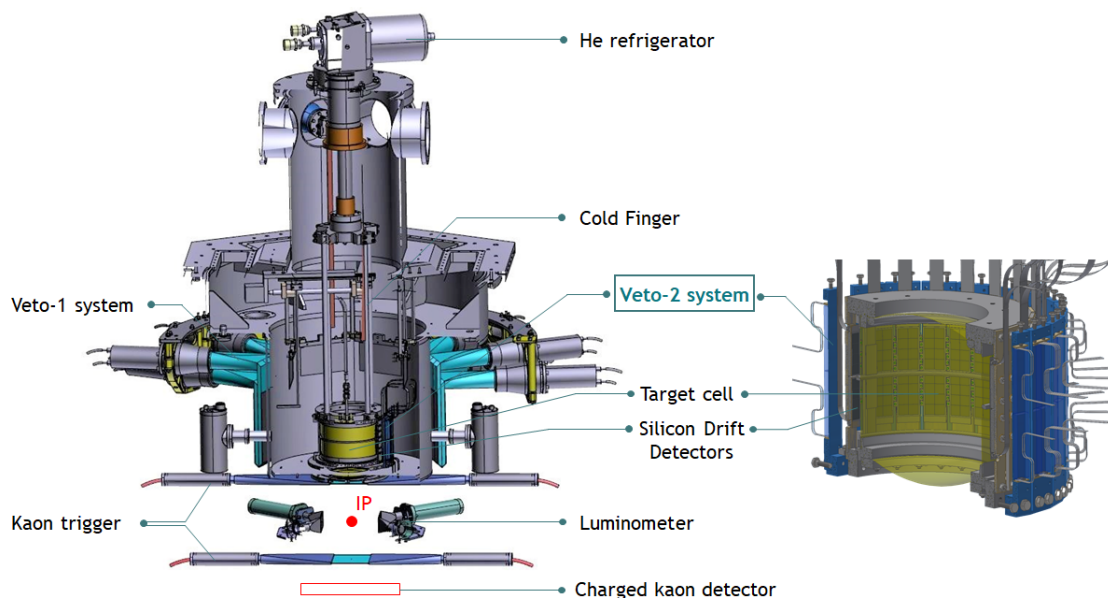


**Figure 4**. Schematic drawing of the SIDDHARTA-2 experimental apparatus installed at DAΦNE. A detailed cross section view of the Veto-2 system (blue) surrounding the SDDs and the target cell (yellow) is shown on the right.

## 3 Veto-2 detector characterisation

Since the Veto-2 system is based on solid-state photodetectors and is installed in a high-radiation environment, radiation damage of the SiPMs is a concern. The Veto-2 was first mounted in DAΦNE during its commissioning phase in 2019, where the background radiation was high due to beam losses and bremsstrahlung. After approximately six months in this environment, the Veto-2 detectors showed signs of radiation damage. Firstly, their dark current had increased by one to two orders of magnitude compared to unirradiated SiPMs at equal bias voltage. Figure 5 shows the current-voltage curves for two SiPMs that were previously installed in DAΦNE (7B1, 7B2) and for two unirradiated ones (55, 53). The increase of dark currents is a well-known phenomenon of radiation damage to SiPMs and its causes are, for example, described in [27].

Secondly, the SiPM signal amplitudes decreased down to the noise level, which was mainly due to the electronic configuration of the HV modules. They operated as constant-current sources, which led to a decrease of the bias voltage to or below the SiPMs' breakdown voltage in an attempt to stabilise the high dark currents. This deterioration of signal made it impossible to distinguish between MIP signals and thermal noise. The modification of the HV modules to constant-voltage
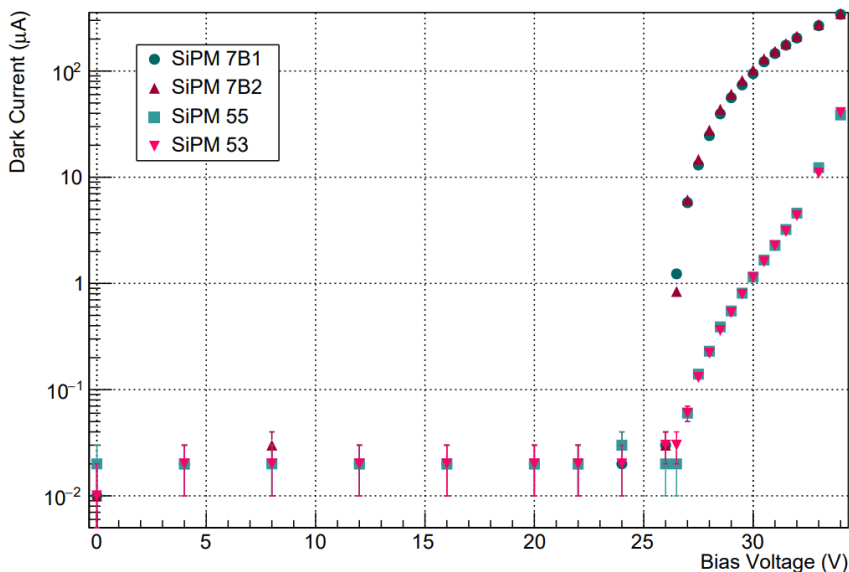
**Figure 5**. Current-voltage curves for two SiPMs irradiated in DAΦNE (7B1, 7B2) compared to two unirradiated SiPMs (53, 55). The irradiated detectors show an increased dark current at equal bias voltage.

sources enables the detectors to operate also for moderate radiation damage. A constant bias voltage is supplied, and a distinction between signals and noise is possible even at high dark currents. This allows for the operation of the Veto-2 system for approximately six months before the need to exchange the SiPMs. For more details refer to [17].

The performance of the Veto-2 system during its operation in the SIDDHARTA-2 apparatus in terms of its efficiency and timing capabilities has been studied. Figure 6 shows the X-ray spectrum accumulated with a helium-4 target for an integrated luminosity of $5\,\mathrm{pb}^{-1}$, after the application of all steps of background suppression. These included the following measures: a coincidence between signals in the two scintillators of the kaon trigger provided a clean kaon signature, and a Time-of-Flight (ToF) measurement by the kaon trigger was used to distinguish kaons from MIPs produced in beam-beam interactions. Finally, the SDD timing was employed to suppress the asynchronous background, while the synchronous background was suppressed by the veto system. The L-X-ray transitions of kaonic helium-4 are clearly visible in the resulting spectrum. In addition, the spectrum shows transitions from kaonic atoms produced in the solid structures of the apparatus, including the support structures, entrance window and walls of the target cell. As described before, the purpose of the Veto-2 system is the suppression of synchronous background in the form of MIPs produced by the absorption of the $K^-$ on the target nucleons. This component can be reduced via an evaluation of the spatial correlation of signals in the SDDs and the corresponding signals in the Veto-2 detectors, in coincidence with the detection of a pair of charged kaons in the kaon trigger. For each SDD cell, eight Veto-2 detectors are considered. They include the four detectors in the unit directly behind the SDD array, as well as the two neighbouring ones. This allows to include inclined or grazing hits due to the broad kaon stopping distribution in the target cell. An SDD signal is discarded as background when one of the Veto-2 detectors corresponding to that SDD cell also registers a hit within a 5 μs window after the kaon trigger.
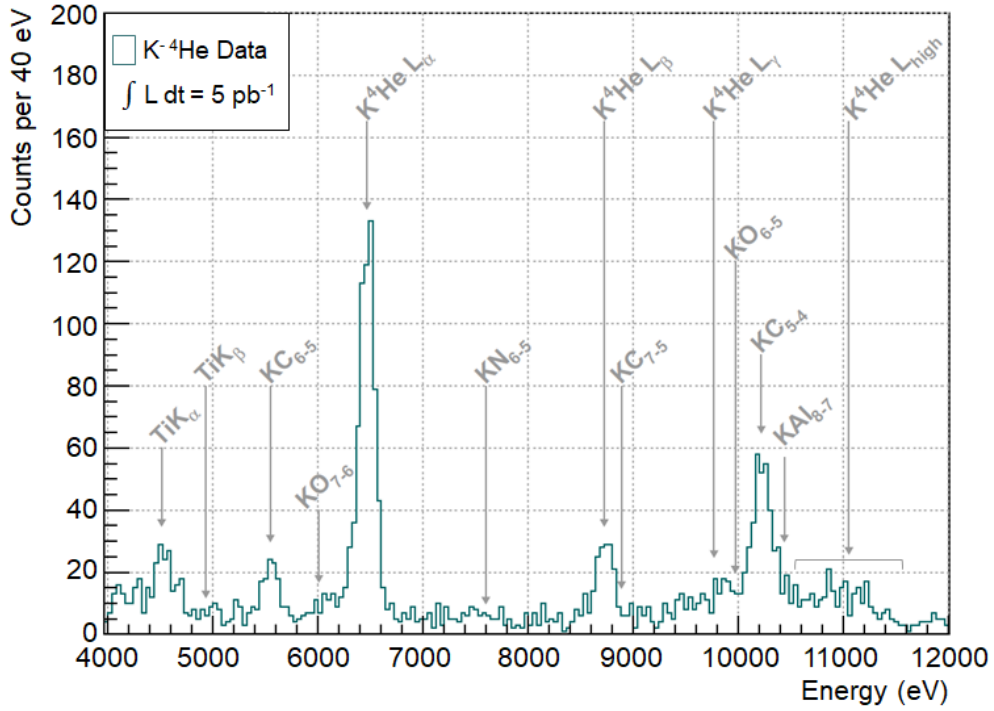
**Figure 6**. X-ray spectrum after background reduction for $5\,\mathrm{pb}^{-1}$ of 1.1% LHeD data.

In this configuration, the efficiency of the Veto-2 system was determined from the helium-4 data collected in 2022. Its intrinsic detection efficiency was studied in 2018 with cosmic rays and found to be > 99% [28, 29]. To select events produced by hadronic background in the data, a coincidence of signals in the SDDs and in one of the two spatially corresponding Veto-1 detectors was required (figure 7). For the efficiency determination, SDD signals with energies >20 keV were selected since they correspond to central MIP hits of the SDDs and thus produce signals in the SDDs, the Veto-2, and the Veto-1. Given the SDD-Veto-1 coincidence, eight Veto-2 detectors were monitored for a signal (see the darker magenta units in the centre in figure 7). The number of events $\Sigma_{\mathrm{Veto\text{-}2}}$ for which one of those eight counters detected a signal was calculated. The efficiency was then determined as the ratio of $\Sigma_{\mathrm{Veto\text{-}2}}$ to the number of coincidences $\Sigma_{\mathrm{Coinc}}$ between SDDs and Veto-1 detectors, and found to be $0.62 \pm 0.01$ (table 1).

The uncertainties on $\Sigma_{\mathrm{Veto\text{-}2}}$ and $\Sigma_{\mathrm{Coinc}}$ were determined according to Poisson statistics, and the final uncertainty was calculated via error propagation. The topological correlation of the detectors in the coincidence used for the analysis is shown in figure 7, which was chosen to consider off-center grazing hits, as described previously. The importance of this geometric correlation is corroborated by the significant decrease of efficiency of the Veto-2 system to $0.23 \pm 0.01$ when only the single Veto-2 detector directly aligned with the respective SDD cell is considered.

**Table 1**. Efficiency of the Veto-2 system within the apparatus.

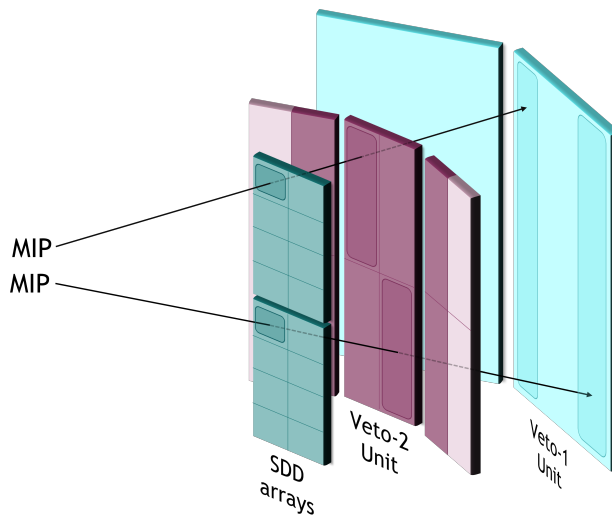| Target | $\Sigma_{\mathrm{Veto\text{-}2}}$ | $\Sigma_{\mathrm{Coinc}}$ | Efficiency |
|---|---|---|---|
| 1.1% LHeD | $7671 \pm 87$ | $12\,422 \pm 111$ | $0.62 \pm 0.01$ |

**Figure 7**. The geometrical approach to determine the efficiency of the Veto-2 system. For each high-energy SDD hit, two Veto-1 detectors were considered and a coincidence of SDDs and Veto-1 was required to select hadronic background events. Given this coincidence, eight Veto-2 detectors (dark magenta) were monitored for a signal.

Compared to its intrinsic detection efficiency of > 99%, the efficiency of the Veto-2 system within the apparatus is substantially lower. This discrepancy can be explained by the presence of an additional component of background to the kaon-correlated hadronic one, originating from beam-beam interactions via the Touschek effect and/or the following bremsstrahlung. This additional background component leads to accidental coincidences in the SDDs and Veto-1 system. In addition to actively suppressing the synchronous background, the Veto-2 system therefore provides a valuable tool to understand the background level and its composition during data acquisition, and to adapt and optimise the performance of the machine and of the setup accordingly.

The performance of the apparatus for X-rays generated by kaonic atoms can be optimised by using the timing information from the Veto-2 system. Since the time resolution of the Veto-2 is $(293 \pm 45)$ ns [29], distinguishing between kaon stops in the target gas and kaon stops in the solid structures of the setup is possible on the basis of timing information, analogously to the Veto-1 system [16]. The solid structures in the setup in particular include the entrance window and side walls of the target cell and the entrance window to the vacuum chamber. The kaon stop in a solid leads to the prompt emission of MIPs, whereas in the target gas the moderation time is much longer. Figure 8 shows the leading edge time distribution of the time-over-threshold signals summed over all 96 Veto-2 channels during the $\text{K}^{-4}\text{He}$ run, requiring a signal in the SDDs. The origin of the double-peak structure was investigated by selecting only events with energies corresponding to transitions from specific kaonic atoms, in particular the kaonic helium-4 $\text{L}_\alpha$ transition, the kaonic carbon ($5 \rightarrow 4$) transition, the kaonic nitrogen ($6 \rightarrow 5$) transition, the kaonic aluminium ($7 \rightarrow 6$) transition, and the titanium $\text{K}_\alpha$ fluorescence line. The timing spectra corresponding to these transitions are shown in the left panels of figure 9. The panels on the right show the correlation between the transition energies and the leading edge timing for these transitions. The two transitions with the highest statistics, i.e. the $\text{K}^{-4}\text{He}$ $\text{L}_\alpha$ and $\text{K}^-\text{C}$ ($5 \rightarrow 4$) transitions, are enclosed in the ellipses. The data
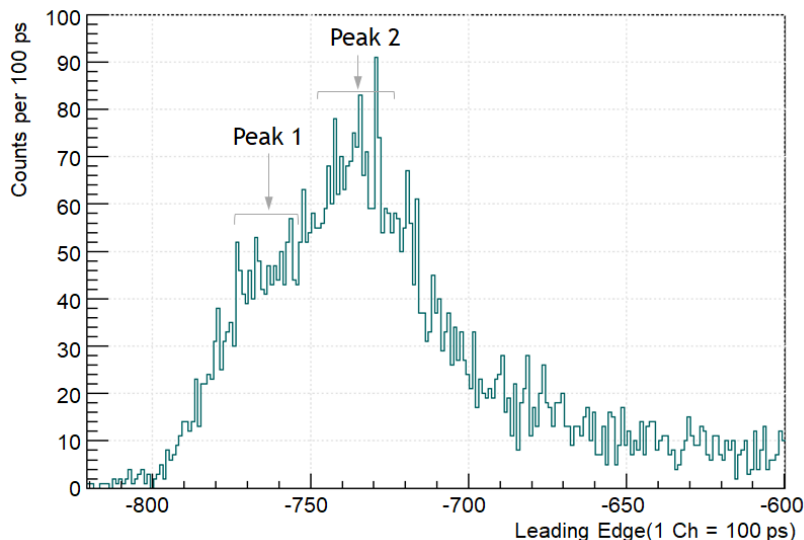
**Figure 8**. Leading edge timing summed for all Veto-2 channels for the 1.1% LHeD run.

indicate a difference in timing depending on the selected transition. The kaonic carbon and nitrogen X-rays originate in the target cell entrance window made of Kapton polyimide ($C_{22}H_{10}N_2O_5$), and thus have faster arrival times than the kaonic helium X-rays produced in the target gas. The titanium fluorescence lines are produced in the top part of the target cell which consists of titanium, and the kaonic aluminium transitions originate from the target cell bottom ring and sidewall frames. The timing information provided by the Veto-2 system can be used to identify the origin of the detected X-ray transitions. It thus provides information on the kaon stopping distribution in the setup, which depends on the configurations of the kaon degrader and target cell entrance window, as well as on the target gas density. This provides additional evidence for the capability of the Veto-2 system to optimise the setup. The timing information can, in particular, be used to optimise components like the kaon degrader, the material and thickness of the target cell entrance window, and the target gas density, and also to monitor their performance as well as any changes to the system during data acquisition.

## 4   Outlook: the Veto-2 background suppression

By utilising the $5 \, \text{pb}^{-1}$ data collected with the helium-4 target, the effect of the Veto-2 system on the signal-to-background ratio was studied. To obtain this ratio, a fit function was applied to the X-ray spectrum. The kaonic helium-4 $L_\alpha$ transition was reproduced in the fit by a Voigtian function (the convolution of a Gaussian and a Lorentzian function). The signal strength was obtained from the amplitude of the fitted Voigtian curve. The background shape was described in the fit by the sum of a constant and an exponential function. Since in the energy region from 7 to 8 keV the background shape is approximately constant, the background level in the $K^{-4}He$ region ($\sim 6.4 \, \text{keV}$) was obtained from the mean value of 50 equidistant points of the background function in this region. Finally, to extract the effect of the Veto-2 system on the signal-to-background ratio, the fit was performed on the X-ray spectrum before and after applying the Veto-2 system suppression (see figure 10). The suppression of hadronic background using the topological correlation between
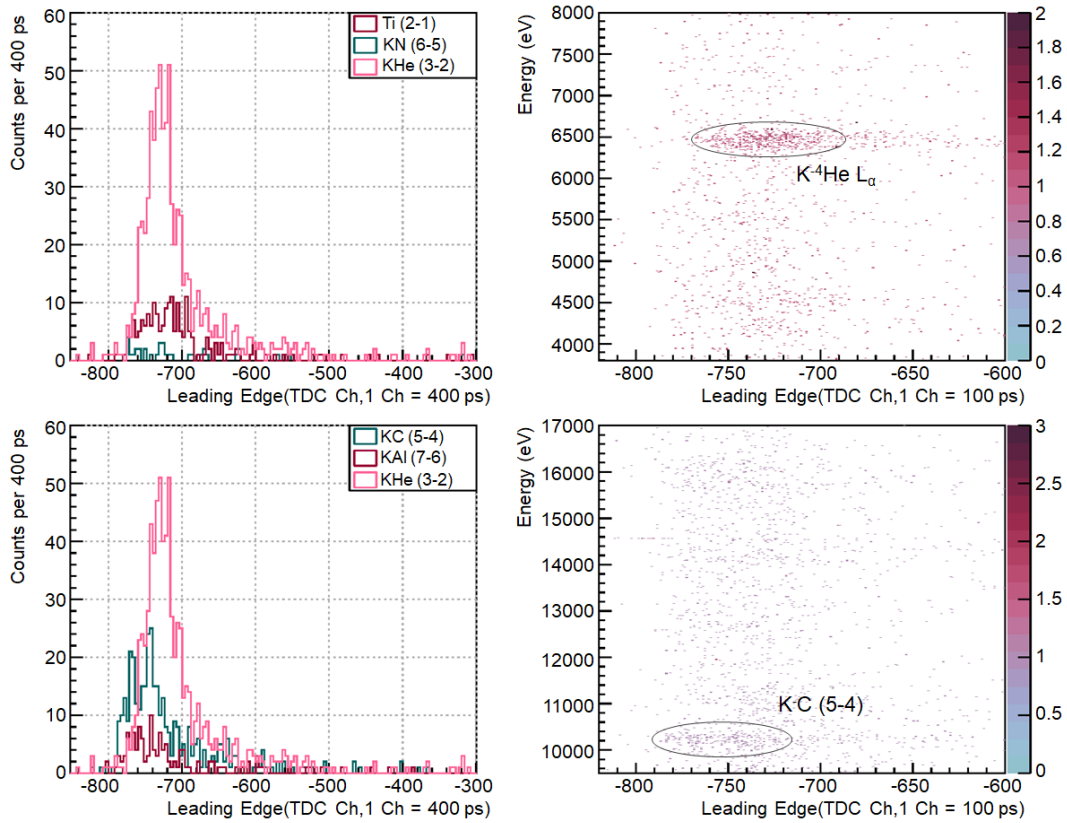
**Figure 9**. *Left:* leading edge timing summed over all Veto-2 channels for selected transitions in various kaonic atoms and fluorescence lines. *Right:* energy-timing scatter plot for the selected transitions. The kaonic helium-4 $L_\alpha$ and kaonic carbon $(5 \rightarrow 4)$ transition clusters are shown by the ellipses, indicating earlier arrival times for the kaonic carbon X-rays than for the X-rays produced in the target gas.

signals in the X-ray detectors and signals in the Veto-2 system leads to an improvement of the S/B of approximately 16% [17]. This value is in agreement with the result of a dedicated SIDDHARTA-2 Monte Carlo simulation based on GEANT4, which predicts an improvement of the S/B due to the Veto-2 system by 17% [30, 31]. This calculation assumed a 1:1 ratio between kaon-correlated and uncorrelated backgrounds, which was observed in the data analysis during this measurement. An additional suppression of the uncorrelated background during the upcoming data taking would amplify the effect of the Veto-2 system on the S/B. This can be achieved by improving the passive shielding around the apparatus, which is planned for the upcoming periods of data taking. For a hypothetical reduction of the uncorrelated background by 70%, the Monte Carlo simulation predicts an improvement of the S/B by 43%. The background suppression provided by the Veto-2 system is crucial for the challenging kaonic deuterium measurement: the $K_\alpha$ X-ray yield in kaonic deuterium is expected to be lower by approximately two orders of magnitude with respect to the $L_\alpha$ yield in kaonic helium-4 [3–6, 32]. Therefore, conserving the strength of the signal, together with an efficient suppression of correlated background, is vital for the success of the $K^-d$ measurement.

Based on the results from the kaonic helium run, the design of the Veto-2 system has recently been updated. As shown by the analysis of the performance of the system, the granularity of the

detectors can be decreased without loss of efficiency. Consequently, the new Veto-2 system features two scintillators of size $13 \times 5 \times 100 \, \text{mm}^3$ per unit instead of the previous four. Each scintillator is read out by two SiPMs. In this way, a coincidence between the signals in the two SiPMs is required, which results in the efficient suppression of electronic or thermal noise. The new version of the Veto-2 system already performed its first run at DAΦNE. After operating for an integrated luminosity of $200 \, \text{pb}^{-1}$ (corresponding to approximately four months), the SiPMs again showed increased dark currents from $110 \, \mu\text{A}$ to $190 \, \mu\text{A}$, due to radiation damage. The currents were originally set to $3 \, \mu\text{A}$ and the overvoltage remained constant. Nevertheless, the first analyses indicate that the Veto-2 system operated efficiently during this time despite the damage, thus certifying the effectiveness of the electronic modifications.
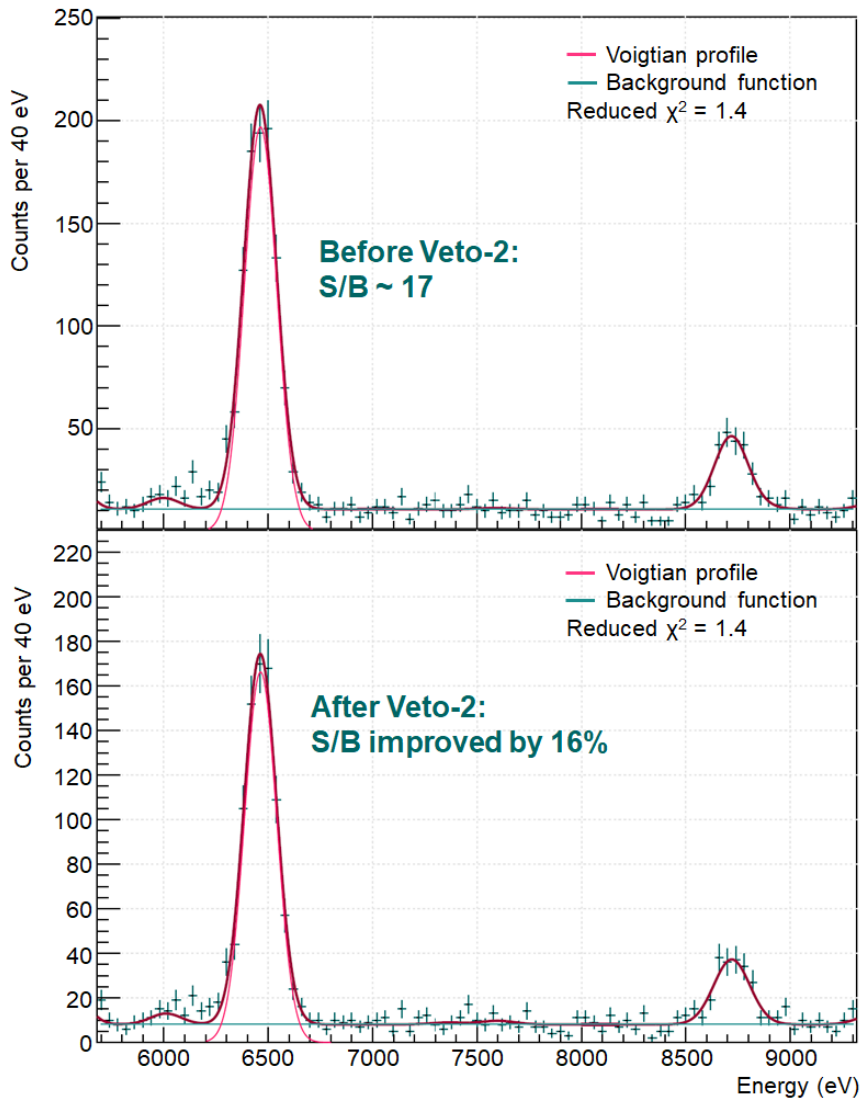


**Figure 10**. Improvement of the S/B due to the Veto-2 system. *Top:* the S/B for the $\text{K}^{-4}\text{He} \, \text{L}_\alpha$ transition before the application of the Veto-2 background suppression. *Bottom:* after the application of the Veto-2 system, the S/B improved by $\sim 16\%$, which is in agreement with the predictions of Monte Carlo simulations.

# 5 Conclusion

The Veto-2 system was characterised during its first successful run at DAΦNE with a helium-4 target in 2022. Despite the challenging conditions at the DAΦNE collider, the Veto-2 was able to efficiently suppress the synchronous background via the topological correlation between signals in the X-ray detectors and signals in the Veto-2 detectors, thus improving the signal-to-background ratio for the kaonic helium-4 $L_\alpha$ transition by $\sim 16\%$. The detection efficiency of the Veto-2 within the SIDDHARTA-2 apparatus was studied and found to be $0.62 \pm 0.01$. In addition to the background suppression, the Veto-2 system has proven to be a very useful tool to evaluate the level of background radiation present during beam time as well as its composition. The timing information provided by the Veto-2 system enables to reconstruct where the kaonic atoms are formed. This information is crucial for the optimisation of the kaon degrader thickness, the entrance window of the target cell, and the target gas density. The challenging measurement of kaonic deuterium by the SIDDHARTA-2 experiment with an optimised Veto-2 system is currently ongoing.

## References

[1] SIDDHARTA collaboration, *Kaonic hydrogen X-ray measurement in SIDDHARTA*, *Nucl. Phys. A* **881** (2012) 88 [arXiv:1201.4635].

[2] C. Curceanu et al., *The modern era of light kaonic atom experiments*, *Rev. Mod. Phys.* **91** (2019) 025006.

[3] SIDDHARTA collaboration, *Preliminary study of kaonic deuterium X-rays by the SIDDHARTA experiment at DAFNE*, *Nucl. Phys. A* **907** (2013) 69 [arXiv:1302.2797].

[4] M. Bazzi et al., *K-series X-ray yield measurement of kaonic hydrogen atoms in a gaseous target*, *Nucl. Phys. A* **954** (2016) 7 [arXiv:1603.00094].

[5] T. Koike, T. Harada and Y. Akaishi, *Cascade calculation of $K^-$-p and $K^-$-d atoms*, *Phys. Rev. C* **53** (1996) 79.

[6] M. Faber et al., *Energy Level Displacement of Excited np State of Kaonic Deuterium In Faddeev Equation Approach*, *Phys. Rev. C* **84** (2011) 064314 [arXiv:1012.3933].

[7] A. Gal, *On the scattering length of the $K^-$d system*, *Int. J. Mod. Phys. A* **22** (2007) 226 [nucl-th/0607067].

[8] M. Döring and U.-G. Meißner, *Kaon-nucleon scattering lengths from kaonic deuterium experiments revisited*, *Phys. Lett. B* **704** (2011) 663 [arXiv:1108.5912].

[9] N.V. Shevchenko, *Near-threshold $K^-$d scattering and properties of kaonic deuterium*, *Nucl. Phys. A* **890-891** (2012) 50 [arXiv:1201.3173].

[10] T. Mizutani, C. Fayard, B. Saghai and K. Tsushima, *Faddeev-chiral unitary approach to the $K^-$d scattering length*, *Phys. Rev. C* **87** (2013) 035201 [arXiv:1211.5824].

[11] T. Hoshino et al., *Constraining the $\overline{K}N$ interaction from the 1S level shift of kaonic deuterium*, *Phys. Rev. C* **96** (2017) 045204 [arXiv:1705.06857].

[12] M. Miliucci et al., *Silicon drift detectors system for high-precision light kaonic atoms spectroscopy*, *Meas. Sci. Technol.* **32** (2021) 095501.

[13] M. Miliucci et al., *Large area silicon drift detectors system for high precision timed x-ray spectroscopy*, *Meas. Sci. Technol.* **33** (2022) 095502.

[14] M. Miliucci et al., *Silicon Drift Detectors' Spectroscopic Response during the SIDDHARTA-2 Kaonic Helium Run at the DAΦNE Collider*, *Condens. Mat.* **6** (2021) 47 [arXiv:2111.01572].

[15] F. Sgaramella et al., *The SIDDHARTA-2 calibration method for high precision kaonic atoms x-ray spectroscopy measurements*, *Phys. Scripta* **97** (2022) 114002 [arXiv:2201.12101].

[16] M. Bazzi et al., *Characterization of the SIDDHARTA-2 second level trigger detector prototype based on scintillators coupled to a prism reflector light guide*, 2013 *JINST* **8** T11003.

[17] M. Tüchler, *Probing the strong interaction with kaonic atom X-ray measurements at low energies*, Ph.D. thesis, University of Vienna, Vienna, Austria (2023).

[18] AdvanSiD Advanced Silicon Detectors, *NUV SiPMs Chip Scale Package (CSP)*, 2015.

[19] C. Sauerzopf et al., *Intelligent Front-end Electronics for Silicon photodetectors (IFES)*, *Nucl. Instrum. Meth. A* **819** (2016) 163.

[20] H. Schneider, private communication, 2023.

[21] M. Skurzok et al., *Characterization of the SIDDHARTA-2 luminosity monitor*, 2020 *JINST* **15** P10010 [arXiv:2008.05472].

[22] P. Moskal et al., *Simulating NEMA characteristics of the modular total-body J-PET scanner — an economic total-body PET from plastic scintillators*, *Phys. Med. Biol.* **66** (2021) 175015 [arXiv:2107.01356].

[23] P. Moskal et al., *Testing CPT symmetry in ortho-positronium decays with positronium annihilation tomography*, *Nat. Commun.* **12** (2021) 5658 [arXiv:2112.04235].

[24] P. Moskal et al., *Positronium imaging with the novel multiphoton PET scanner*, *Sci. Adv.* **7** (2021) eabh4394.

[25] S. Niedźwiecki et al., *J-PET: a new technology for the whole-body PET imaging*, *Acta Phys. Polon. B* **48** (2017) 1567 [arXiv:1710.11369].

[26] Particle Data Group collaboration, *Review of Particle Physics*, *PTEP* **2022** (2022) 083C01.

[27] E. Garutti and Y. Musienko, *Radiation damage of SiPMs*, *Nucl. Instrum. Meth. A* **926** (2019) 69 [arXiv:1809.06361].

[28] M. Tüchler et al., *A charged particle veto detector for kaonic deuterium measurements at DAΦNE*, *J. Phys. Conf. Ser.* **1138** (2018) 012012.

[29] M. Tüchler, *A charged particle veto detection system for kaonic deuterium measurements at DAΦNE*, M.Sc. thesis, University of Vienna, Vienna, Austria (2019).

[30] GEANT4 collaboration, *GEANT4 — a simulation toolkit*, *Nucl. Instrum. Meth. A* **506** (2003) 250.

[31] M. Cargnelli, M. Iliescu and D. Sirghi, private communication.

[32] D.L. Sirghi et al., *New measurements of kaonic helium-4 L-series X-rays yields in gas with the SIDDHARTINO setup*, *Nucl. Phys. A* **1029** (2023) 122567.